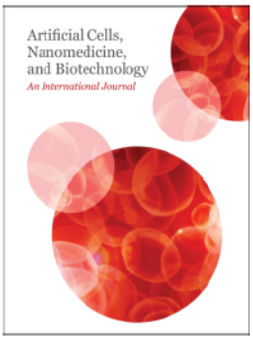

Taylor & Francis
Taylor & Francis Group

Artificial Cells, Nanomedicine, and Biotechnology
An International Journal

ISSN: (Print) (Online) Journal homepage: www.tandfonline.com/journals/ianb20

Exploring fibroblast interactions on nanocrystalline surfaces in physiological environments through a phenomenological lens

R.D.K Misra & Aladin M. Boriek

To cite this article: R.D.K Misra & Aladin M. Boriek (2024) Exploring fibroblast interactions on nanocrystalline surfaces in physiological environments through a phenomenological lens, Artificial Cells, Nanomedicine, and Biotechnology, 52:1, 229-237, DOI: 10.1080/21691401.2024.2338127

To link to this article: https://doi.org/10.1080/21691401.2024.2338127

Published online: 08 Apr 2024.

ARTIFICIAL CELLS, NANOMEDICINE, AND BIOTECHNOLOGY
2024, VOL. 52, NO. 1, 229–237
https://doi.org/10.1080/21691401.2024.2338127

Taylor & Francis
Taylor & Francis Group

Exploring fibroblast interactions on nanocrystalline surfaces in physiological environments through a phenomenological lens

R.D.K Misra[a] and Aladin M. Boriek[b]

[a]Department of Metallurgical, Materials, and Biomedical Engineering, University of TX at El Paso, El Paso, TX, USA; [b]Departments of Medicine and Molecular Physiology and Biophysics, Baylor College of Medicine, Houston, TX, USA

ABSTRACT

The cytological behaviour and functional dynamics (adhesion, spreading, synthesis of proteins) of fibroblasts when interacting with biomedical surfaces are intricately influenced by the inherent nature of surface (nanocrystalline or microcrystalline), where the nanocrystalline (NC) surface is preferred in relation to the microcrystalline (MC) surface. This preference is a direct consequence of the distinct differences in physical and chemical characteristics between NC and MC surfaces, which include crystal boundary bio-physical attributes, electron work function, surface energy, and charge carrier density. The observed variances in cytological behaviour at the interfaces of NC and MC bio-surfaces can be attributed to these fundamental differences, particularly accounting for the percentage and nature of crystal boundaries. Recognising and understanding these physical and chemical characteristics establish the groundwork for formulating precise guidelines crucial in the development of the forthcoming generation of biomedical devices.

HIGHLIGHT POINTS

The significance of nanoscale surface in favourably modulating the cellular functionality is described with the aim to provide the solution to the current day challenges in the biomedical arena. Furthermore, the perspective presented advances the nano-bio science forward by implying that the nanoscale structure induces chemical and physical changes that can be considered responsible for favourable modulation of cellular activity in the living organism.

ARTICLE HISTORY
Received 13 March 2024
Accepted 25 March 2024

KEYWORDS
Biomedical stainless steel; nanocrystalline; crystal boundary attributes; biological functionality

Fabrication and characterization of nanocrystalline surfaces to investigate fibroblast interactions

Titanium alloys and austenitic stainless steels are predominantly used for the fabrication of biomedical devices [1–5]. In some instances, biomedical devices exhibit premature failure, which is generally a consequence of inadequate build-up of tissue around the device. This leads to loosening of the biomedical device and is further facilitated by diminished cell–surface interactions. Additionally, factors such as wear and generated debris also contribute significantly to biomedical device failure. This impacts the immune response of the physiological system, which leads to inflammation, necrosis, and the loss of bone surrounding the implant [1–5]. Keeping this in mind, the nanocrystalline biomedical device system is a promising and viable approach for fabrication of futuristic biomedical devices [4]. This aspect is illustrated below, where the cytological interactions on NC surfaces are observed, which facilitate tissue growth and mineralization. Moreover, the enhanced strength associated with NC materials serves as an advantage, facilitating enhanced wear resistance and reduced device weight since a thinner biomedical device would meet requisite specifications [1–5].

To obtain nanocrystalline and ultrafine-crystalline structures, methods such as heat treatment [4–6], powder metallurgy [7], and sintering [8,9] have been adopted, which modulate cytological functions and extend the operational lifespan of medical devices [8–15]. While laboratory-scale severe plastic deformation methods such as equal channel angular pressing (ECAP) [15–18], accumulative roll bonding (ARB) [19–21], high-pressure torsion (HPT) [22–25], multiple compression [26], and upsetting extrusion [27] have shown success, they often compromise ductility, a crucial factor for biomedical device fabrication. A high strength-high ductility combination is necessary for a prolonged lifespan in any metallic device [28–31]. To address this necessity, Misra's group developed an ingenious concept of phase reversion with a specific focus on stainless steel to achieve a nanocrystalline structure within the bulk alloy [32–34]. This concept involves cold-reducing stainless steel by approximately ~60–80%, inducing a phase transformation from face-centred austenite to body-centred martensite. Subsequent short-term

CONTACT R.D.K. Misra dmisra2@utep.edu Department of Metallurgical, Materials, and Biomedical Engineering, University of TX at El Paso, El Paso, TX, USA

heat treatment at higher temperatures of 700–800 °C for short durations of 10–100 s reverts the martensite phase to austenite [1–3,32–34]. Notably, the resultant crystalline structure is influenced by the degree of cold deformation and the specifics of temperature-time heat treatment. Figure 1 illustrates a comparative analysis between the nanocrystalline structure and conventional microcrystalline structures. The nanocrystalline structure, achieved through the phase reversion process, remarkably preserves ductility while enhancing strength, defining a paradigm of high strength-high ductility combination within nanocrystalline stainless steel [33]. This augmented strength not only contributes to wear resistance but also extends the material's lifespan, while the retained ductility holds promise for biomedical device fabrication [1–3,32–34].

The primary aim of this study is to elucidate fundamental insights into the distinctive characteristics of nanocrystalline surfaces, characterized by crystal sizes within the nanoscale range and crystal boundaries exceeding 50%. We aim to compare these characteristics with those of microcrystalline surfaces, characterized by crystal sizes in the microscale range with approximately ~2–3% crystal boundaries. We hypothesize that these differences play a key role in enhancing the adhesion of fibroblast cells to the NC surface, leading to enhanced cellular spreading, synthesis of key proteins, and mineralisation processes. In this regard, we initially provide an overview by summarising the findings from prior studies on the cytological functions such as cell adhesion, proliferation, protein synthesis, mineralisation, and cell differentiation on both NC and MC surfaces. This is followed by a discussion of our viewpoints regarding the relationship between the chemical and physical attributes of these surfaces and their potential impact on cellular functions. We postulate that these attributes significantly influence the observed differences in cellular activities between the NC and MC surfaces. This investigation seeks to uncover the relationship between surface properties and cellular behaviours, ultimately providing valuable insights into the molecular mechanisms governing biological functions. The understanding of these physical and chemical attributes is expected to provide a strong rationale for further mechanistic studies, the results of which will be reported in subsequent reports.

Experimental methodology to study cellular interactions between the nanoscale surface and the biological environment

The phase reversion concept enables varying crystal size to be obtained in the bulk alloy [1–3,32–34]. The data in Figure 1 demonstrate the relationship between nanocrystalline size, determined by varying cold reduction percentages and temperature heat treatments, and corresponding strength and mechanical percent elongation. This is contrasted with the characteristics of the microcrystalline counterpart. Multiple micrographs were used to derive the average crystal size, while the mechanical properties were assessed following the guidelines set by the ASTM standard. The average crystal size of MC steel was 22 ± 3 µm with a yield strength of 350 ± 5 MPa and elongation of ~40%. On the contrary, the nanocrystalline steel was characterized by average crystal size of 90 ± 8 nm, yielding a strength of 800 ± 7 MPa and elongation of ~38%. These properties exhibit exceptional performance for bulk nanocrystalline stainless steel [1–3,32–34].

Here, we provide a concise overview of the experimental protocol employed to explore biological functions and surface interactions with cells. A comprehensive and detailed description can be found elsewhere [35–40].

Preparation of nanocrystalline and microcrystalline surfaces

Recognising the substantial impact of surface roughness on cell adhesion, we carefully ensured that the surfaces under investigation for cellular functions exhibited near atomic-scale roughness. This was achieved by sequentially polishing the surface using various grades of SiC paper, resulting in a final polish using colloidal silica in water. The average arithmetic mean roughness (Ra), measured across a 3 µm × 3 µm scan

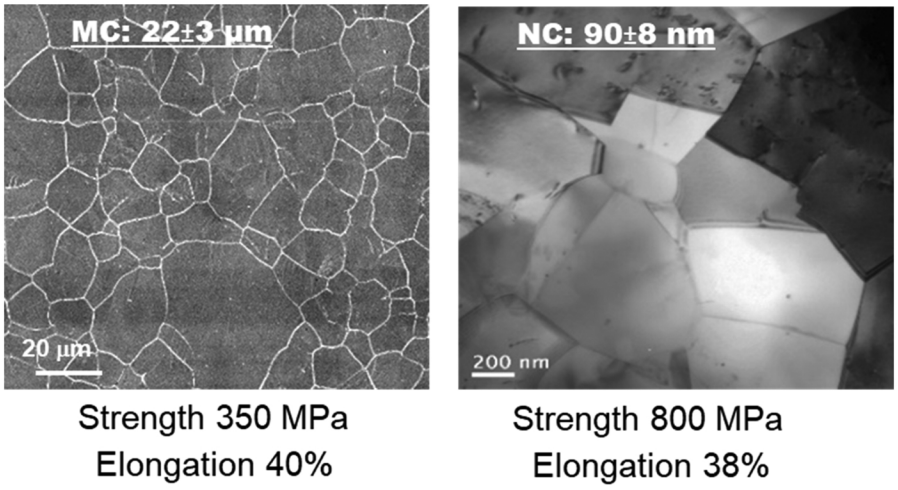

Figure 1. Light micrograph of microcrystalline (MC) and TEM micrograph of nanocrystalline (NC) biomedical stainless steels (adapted from references 1–3).

area, was found to be 1.45 ± 0.21 nm for MC stainless steel and 1.52 ± 0.29 nm for NC stainless steel [35–40].

Cell culture

The study utilized a mouse fibroblast cell line (L-cell-L929 ATCC, USA) to investigate cytological functions on NC and MC surfaces. These fibroblasts were cultured in Eagle's minimum essential medium (Invitrogen Corporation, USA) supplemented with 10% horse serum, penicillin (100 U mL^{-1}), and streptomycin (100 µg mL^{-1}). The surfaces were prepared by mechanically polishing them to achieve nanometric roughness and sizing them to 1 cm^2. Following cleaning in an ultrasonic bath with ethanol and deionized water, each surface was individually wrapped in gauze and sterilized in an autoclave. Fibroblasts at 80–85% confluence, derived from T-flask cultures through trypsinization, were used to seed onto the polished samples [3,37,40]. Fibroblast cells were washed with phosphate-buffered saline (PBS), then incubated with 0.25% trypsin/0.53 mM EDTA for 5-7 min to detach them from the Petri dish. After dispersion in trypsin/EDTA, cells were transferred to a centrifuge tube and spun at 2000 rpm for 5 min. The resulting cell pellet was re-suspended in a culture medium and appropriately diluted to obtain the required cell concentration. Following this preparation, sterilized steel discs were placed in a 24-well plate and incubated with the cell suspension at 37 °C in a humidified atmosphere containing 5% CO_2 and 95% air. For control experiments, polystyrene 24-well culture plates were used [1–3,35–40].

Adhesion of fibroblasts

The adhesion and density of fibroblasts on NC and MC surfaces were assessed using fluorescent labelling of nucleic acids with a fluorescence microscope (Nikon E600). Fibroblasts (10,000 cells/cm^2) were seeded on NC and MC surfaces and left at 37 °C in an incubator with 5% CO_2 and 95% air for varying durations. Following incubation, the fibroblasts were stained with the nucleic acid dye (Hoechst 33342). The discs containing the seeded cells were washed twice with PBS and then incubated in a solution of 10 µg dye/ml PBS at 25 °C for 10 min before observation under a fluorescence microscope with excitation and emission wavelengths of 346/442 nm, respectively [1–3,35–40].

Response of fibroblasts to MC and NC surfaces

The adhesion and cell density of fibroblasts differed significantly between the NC and MC surfaces (Figure 2). Fibroblasts showed notably higher adherence and cell density on the NC surface compared to the MC surface. This trend was consistent with increased metabolic activity observed *via* mitochondrial reduction in the MTT assay, indicating superior cytocompatibility of the NC surface. Fluorescence micrographs of fibroblasts stained with nucleic acid-specific dye supported this finding (Figure 2) [1–3,35–40]. The variations in fibroblast adhesion density between the NC and MC surfaces were not attributed to cell development or surface adaptation over time [1–3,37,40].

Interestingly, SEM images revealed distinct differences in fibroblast morphology (Figure 3). On the NC surface, fibroblasts displayed widespread cellular with a star-like morphology after approximately 24 h of cell culture. In contrast, while spreading occurred on the MC surface, it was less extensive compared to the NC surface. Overall, fibroblasts exhibited greater spreading on the NC surface, indicating a preferable interaction compared to the MC surface [1–3,37,40].

The synthesis and expression of key proteins (fibronectin, actin, and vinculin) on both surfaces provided further insights into fibroblast interaction. The observations (Figures 2–7) confirmed that the NC surface favoured interaction with surrounding cells, leading to some clumping of fibroblasts [3,37,40].

Confocal microscopy combining cytoskeletal elements and the nucleus (Figure 7) highlighted stronger expression levels of vinculin focal contacts and actin stress fibres on the NC surface compared to the MC surface. This indicated a more intense interaction of fibroblasts with the NC surface in the cellular environment [3,37,40].

Biophysical attributes and the relationship with the interaction of fibroblasts with NC and MC surfaces

To understand the contrasting cytological functions of NC and MC surfaces, we begin by defining a key biophysical

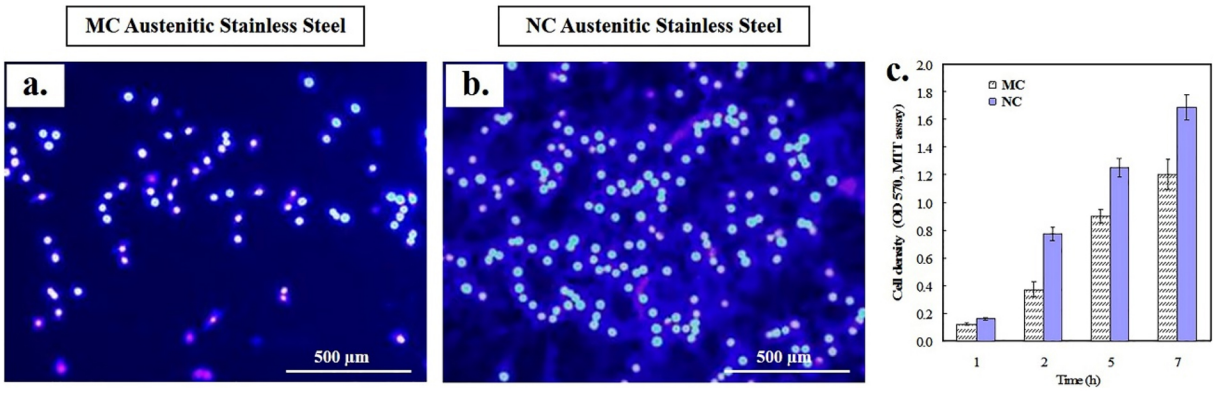

Figure 2. Fluorescence microscopy of fibroblasts nuclei with Hoechst 33258 after 24 h culture on: (a) MC and (b) NC surfaces. NC surface shows higher cell density (b) with abundant extracellular matrix formation as compared to MC (a) surface. (c) Histograms showing higher initial cell density and viability of fibroblasts on NC and MC surfaces using MTT assay (adapted from references 3, 37, 40).

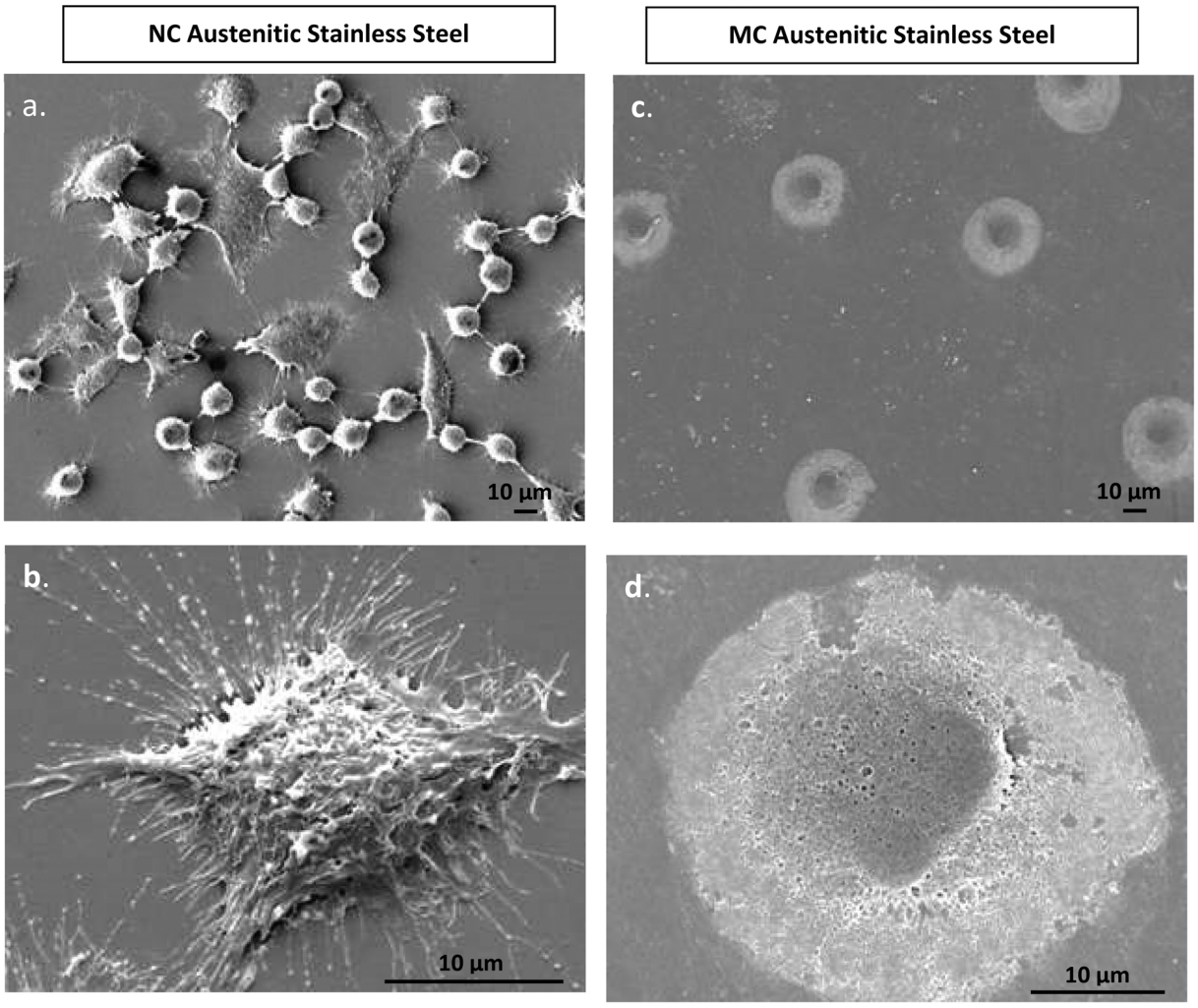

Figure 3. Fibroblasts attachment morphology at 1 h on NC (a, b) and MC austenitic stainless steel (c, d). At low magnification, cells on NC exhibited greater number of attached cells and numerous cellular extensions with thicker extracellular matrices compared to the CG surface. Cells on CG surface is spherical. High magnification micrographs (b, d), cell show higher extent of spreading on NC surface than on MC austenitic stainless steel. Cells on NC austenitic stainless steel show numerous cellular extensions are indicative of extensive attachment and interaction with the substrate (adapted from references 37, 40).

parameter: the average crystal boundary length per surface area. Analysing several micrographs in Figure 1 revealed this parameter to be approximately ~15.5 µm/µm^2 for NC and ~0.14 µm/µm^2 for MC surfaces. Next, considering the typical width (~10–20 µm) and length (~80–100 µm) of fibroblasts, we observe that on the NC surface, a fibroblast cell spans approximately 100–200 crystals in width and 900-1000 crystals in length. Conversely, on the MC surface, a fibroblast extends across only a few crystals in width and approximately 10-15 crystals in length. In brief, the NC surface, rich in crystal boundaries (>50%), accommodates a significantly larger area covered by fibroblasts (1612 µm^2) compared to the MC surface (984 µm^2). To clarify these findings, we combined an important bio-physical parameter [41]—average crystal boundary/cell—with the cellular functionality, i.e. the average area of NC or MC surface covered by fibroblasts. This combination provided the average crystal boundary length per cell. Table 1 summarizes these biophysical parameters and establishes a relationship between these characteristics and the interaction of surfaces with fibroblasts. The table clearly indicates that the average length of crystal boundary/cell occupied by fibroblasts on the NC surface is considerably greater than that on the MC surface. Remarkably, the average intercept length of ~ 50 nm of the NC surface mirrors the average separation distance of endothelial cells (~40 nm) [42].

The relevance of NC surface in the context of cellular interactions

The findings summarised above suggest a clear preference for the NC surface in promoting fibroblast adhesion, proliferation, and key protein synthesis (fibronectin, actin, vinculin) when compared to the MC surface. This preference holds true for similar roughness and an identical microstructural constituent (i.e. austenite phase). This leads us to enunciate that the observed differences in cellular interaction on the NC and MC surfaces stem from disparities in their physical and chemical characteristics. Notably, factors like surface energy, electron work function, surface charge density, and the physical and chemical attributes of crystal boundaries discussed above contribute to these differences. Understanding these distinctions is crucial in customizing the biological functionality of biomedical devices.

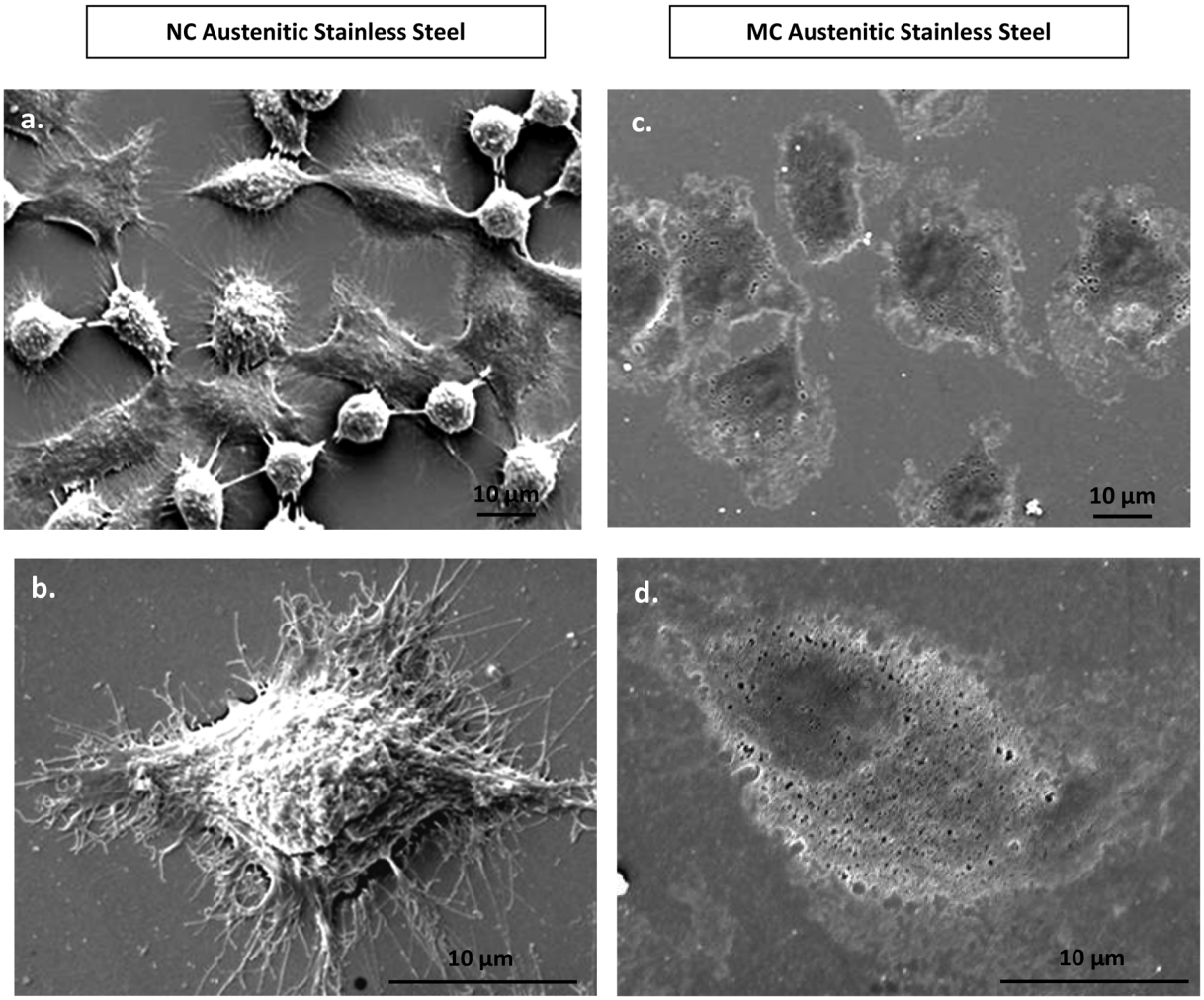

Figure 4. Scanning electron micrographs of fibroblasts morphology at 24 h on NC (a, b) and MC austenitic stainless steel (c, d). Fibroblasts grown on NG/UFG and CG surfaces are significantly different. After 24 h culture, fibroblasts on NC surface exhibit more extensive spreading, interconnectivity and thicker extracellular matrices as compared to MC surface (adapted from references 37, 40).

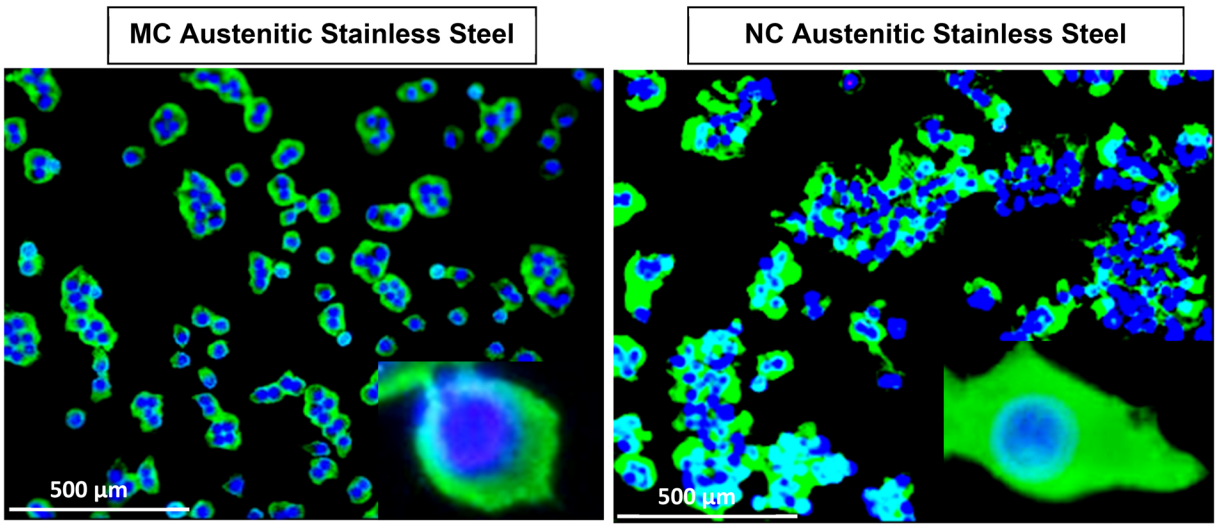

Figure 5. Fluorescence micrographs representing immunocytochemistry of fibronectin expressed by fibroblasts after incubation for 2 days on (a) MC and (b) NC stainless steel surface. A higher fluorescence intensity and expanded network of fibronectin expression along with a higher cell density is observed labelling of cell nuclei with DAPI. Inset is the magnified view of the cell (adapted from references 3, 37, 40).

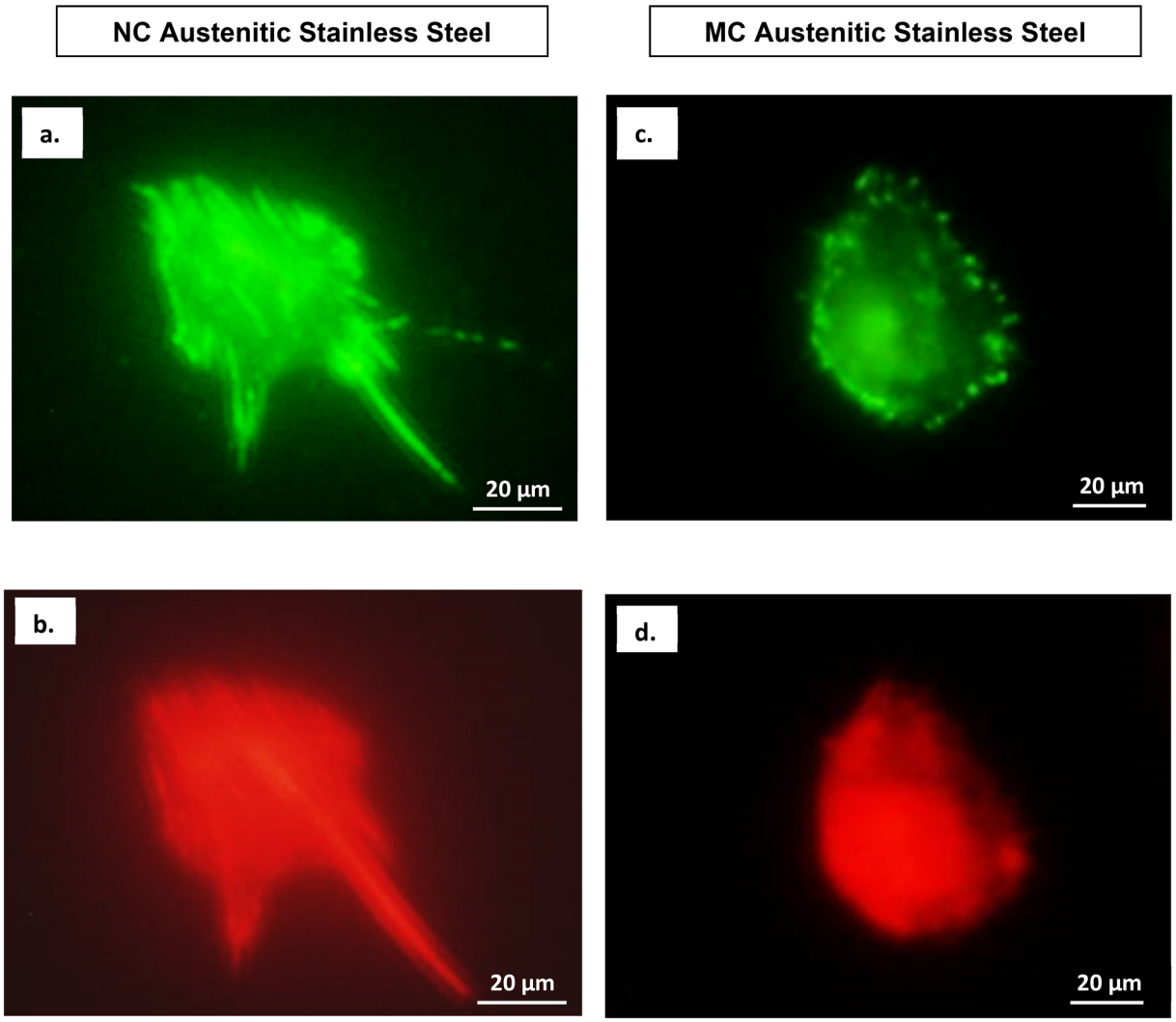

Figure 6. Focal contacts and actin stress fibres of fibroblasts after 2 days culture on MC (a,b) and NC (c,d) stainless steel surfaces. Vinculin (a, c) staining shows a larger number of focal contact sites in fibroblasts grown on the surface of NC(c) compared to cells grown on MC surface (a). The higher number of focal adhesion points corresponded well with a higher number of actin stress fibres on NC surface (d) compared to MC surface (b) (adapted from references 3, 37, 40).

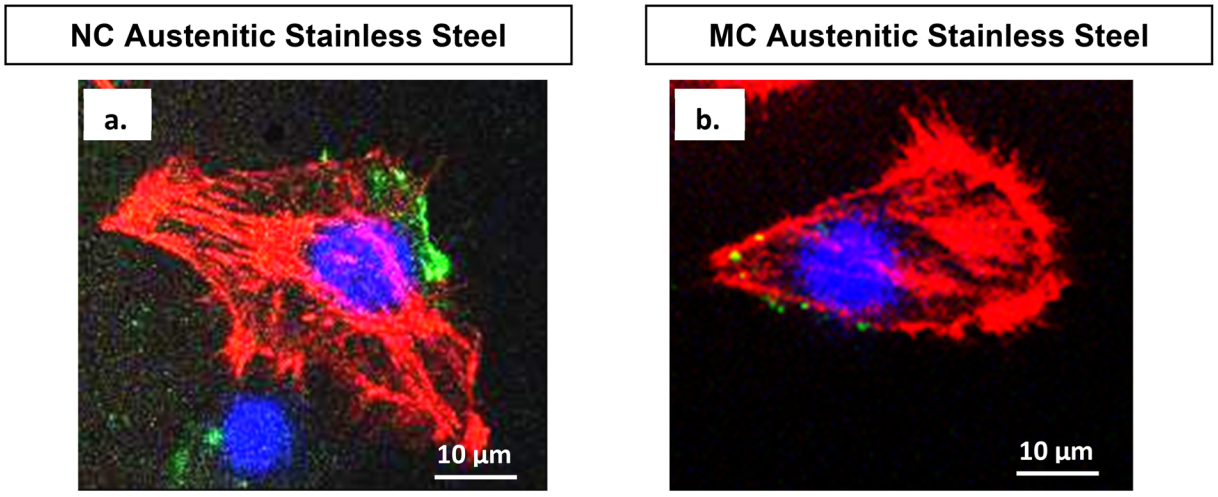

Figure 7. Confocal micrographs show combined distribution of cytoskeletal organisation and focal adhesion contacts. Actin (red), vinculin (green) and nucleus (blue) in fibroblasts cultured for 2 days on NC (a) and MC (b) stainless steel surfaces. The focal contact sites where vinculin is linked at the actin leading edges, which connect cells to the steel surface (adapted from references 37, 40).

Table 1. The significance and global contribution of crystal boundaries, bio-physical characteristics, and average crystal boundary length/cell for nanocrystalline and microcrystalline surfaces.

	The average area of the surface covered by a fibroblast (μm^2)	Average total crystal boundary length/surface area ($\mu m/\mu m^2$)	Average crystal boundary length/cell (μm)
NC	1612.7	15.5	24996
MC	984.5	0.14	138

Our ongoing study investigates the physical and chemical characteristics of biomedical surfaces concerning crystal size. This exploration aims to unravel the molecular mechanisms dictating fibroblast interaction across various crystalline surfaces. Central to our investigation is unravelling how a surface's physical and chemical attributes influence cellular functionality. Clarifying and revealing the mechanism by which the NC surface promotes biological processes such as adhesion, proliferation, and protein synthesis holds the potential for a transformative understanding that could significantly impact the tailoring of surface functionality in biomedical devices.

The insights mentioned above will significantly advance nano-bio science forward by unravelling the understanding of how nanoscale structures induce chemical and physical changes that are responsible for favourable modulation of cellular activity within living organisms. The discovery that nanostructures can enhance cell adhesion through these physical and chemical changes without introducing additional chemical functionalities on the surface represents a significant advancement beyond guiding the customization of cellular functionality at the bio-nano surface.

Ongoing studies into the physical and chemical attributes hold potential for several contributions: (i) Revealing a mechanism explaining how the NC surface induces changes in surface chemistry, surface energy, and electron work functions, thereby impacting cellular functionality. (ii) Elucidating mechanisms involving measurable changes in the crystal boundary state/energy caused by the NC surface compared to the MC surface, and how these changes influence cell adhesion and biological functionality. (iii) Uncovering the mechanism guided by the relationship between the high density of crystal boundaries with high crystal boundary energy and the electronic properties of the NC surface. This exploration aims to enhance our fundamental understanding of how this relationship contributes to the high cell adhesion ability of the NC surface. (iv) Elucidating the relationship between the adhesive force or adhesion energy of the NC surface and its electronic properties, providing a foundational understanding of how this mechanism regulates cell adhesion.

Potential long-term outcomes and benefits to the biomedical field

Understanding the interaction between cells and surfaces can aid in developing surfaces capable of exhibiting specific physical and chemical properties. These surfaces could potentially facilitate targeted biological responses that are critical for optimizing the design of biomedical devices. This understanding can be directly applied to various metallic (like Ti- and Co-based alloys) and non-metallic systems (including ceramics and polymer nanocomposites). This shared structure-property relationship influences osseointegration and the replacement or reconstruction of hard tissues. Biomedical alloys like Ti and Co can undergo severe plastic deformation (e.g. high-pressure torsion) in a manner like the phase reversion concept to attain a NC structure. Exploring how nano-structuring affects cellular functions could significantly advance tissue engineering.

Understanding cell-surface interactions is vital for nanoscale substrate patterning and potentially innovating new biological electromechanics and microfluidic systems at the nanotechnology level. For example, integrating NC elements into microfluidic devices has the potential to broaden their applications to include cell differentiation, sorting, and selective staining. In addition, optimizing the processing of NC implants to modulate biological functionality and enhance wear resistance could enable the customization of surface properties. This customisation could influence cellular behaviours by promoting optimal responses from surrounding tissues, thus enhancing implant functionality.

Acknowledgments

R.D.K. Misra and Aladin M. Boriek are grateful to the National Science Foundation for financial support through grant # CBET 2224942 (Program Manager: Dr. Nora F. Savage).

Author's contribution

Conceptualisation - R.D.K.M.; Writing – original draft preparation – R.D.K.M.; Writing, review, and editing – A.M.B. The authors have read and agreed to the submitted version of the manuscript.

Disclosure statement

No potential conflict of interest was reported by the author(s).

Funding

Funding for this manuscript was supported through grant # CBET 2224942 (Program Manager: Dr. Nora F. Savage).

ORCID

R.D.K Misra http://orcid.org/0000-0002-0918-8180
Aladin M. Boriek http://orcid.org/0000-0002-1467-5629

Data availability

Given that it is an overview article with a perspective, data availability is not applicable. The authors have done their best in citing the relevant articles.

References

[1] Misra RDK, Boriek A. Mechanistic understanding of the interaction of cells with nanostructured surfaces within the framework of bio-

logical functions. Materials Technology – Advanced Performance Materials. 2023;38(1):2216529. doi: 10.1080/10667857.2023.2216529.
[2] Misra RDK. On the relationship between grain boundary attributes with cells in the physiological environment. Mater Lett. 2023;344:134453. doi: 10.1016/j.matlet.2023.134453.
[3] Misra RDK, Enchinton A. The global contribution of crystal boundaries and bio-physical characteristics in the understanding of fibroblasts with the nanoscale surface. Mater Technol, in Press. 2024;39(1) doi: 10.1080/10667857.2024.2326331.
[4] Balasundaram G, Webster T. Increased osteoblast adhesion on nano-grained titanium modified with KRSR. J Biomed Mater Res A. 2007;80(3):602–611. doi: 10.1002/jbm.a.30954.
[5] Willman G. Coating of implants with hydroxyapatite-material connections between bone and metal. Adv Eng Mater. 1999;1:95–105.
[6] Kay S, Thapa A, Haberstroh KM, et al. Nanostructured polymer/nanophase ceramic composites enhance osteoblast and chondrocyte adhesion. Tissue Eng. 2002;8(5):753–761. doi: 10.1089/10763270260424114.
[7] McManus AJ, Doremus RH, Siegel RW, et al. 'Evaluation of cytocompatibility and bending modulus of nanoceramic/polymer composites. J Biomed Mater Res A. 2005;72(1):98–106. doi: 10.1002/jbm.a.30204.
[8] Webster TJ, Ergun C, Doremus RH, et al. Enhanced function of osteoblast on nanophase ceramics. Biomaterials. 2000;67:1803–1810.
[9] Webster TJ, Siegel RW, Bizios R. Osteoblast adhesion on nanophase ceramics. Biomaterials. 1999;20(13):1221–1227. doi: 10.1016/s0142-9612(99)00020-4.
[10] Thapa A, Webster TJ, Haberstroh KM. Polymers with nano-dimensional surface features enhance smooth muscle cell adhesion. J Biomed Mater Res A. 2003;67(4):1374–1383. doi: 10.1002/jbm.a.20037.
[11] Webster TJ, Smith TA. Increased osteoblast function on PLGA composites containing nanophase titania. J Biomed Mater Res A. 2005;74(4):677–686. doi: 10.1002/jbm.a.30358.
[12] Faghihi S, Zhilyaev AP, Szpunar JA, et al. Nanostructuring of a titanium material by high-pressure torsion improves pre-osteoblast attachment. Adv Mater Res. 2007;19(8):1069–1073. doi: 10.1002/adma.200602276.
[13] Faghihi S, Azari F, Zhilyaev AP, et al. Cellular and molecular interactions between MC3T3-E1 pre-osteoblasts and nanostructured titanium produced by high-pressure torsion. Biomaterials. 2007;28(27):3887–3895. doi: 10.1016/j.biomaterials.2007.05.010.
[14] Song R, Ponge D, Raabe D, et al. Microstructure and crystallographic texture of an ultrafine-grained C-Mn steel and their evolution during warm deformation and annealing. Acta Mater. 2005;53(3):845–858. doi: 10.1016/j.actamat.2004.10.051.
[15] Humphreys FJ, Prangnell PB, Bowen JR, et al. Developing stable fine-grain microstructures by large strain deformation. Philosophical Transactions of the Royal Society of London A. 1999;357(1756):1663–1681. doi: 10.1098/rsta.1999.0395.
[16] Pithan C, Hashimoto T, Kawazoe M, et al. Microstructure and texture evolution in ECAE processed A5056. Mater Sci Eng, A. 2000;280(1):62–68. doi: 10.1016/S0921-5093(99)00657-7.
[17] Zhu YT, Lowe TC, Langdon TG. Performance and applications of nanostructured materials produced by severe plastic deformation. Scr Mater. 2004;51(8):825–830. doi: 10.1016/j.scriptamat.2004.05.006.
[18] Park KT, Kim YS, Shin DH. Microstructural stability of ultrafine-grained low-carbon steel containing vanadium fabricated by intense plastic straining. Metall Mater Trans A. 2001;32(9):2373–2381. doi: 10.1007/s11661-001-0211-x.
[19] Tsuji N, Saito Y, Utsunomiya H, et al. Ultra-fine grained bulk steel produced by accumulative roll-bonding (ARB) process. Scr Mater. 1999;40(7):795–800. doi: 10.1016/S1359-6462(99)00015-9.
[20] Saito Y, Utsunomiya H, Tsuji N, et al. Novel ultra-high straining process for bulk materials-development of the accumulative roll-bonding (ARB) process. Acta Mater. 1999;47(2):579–583. doi: 10.1016/S1359-6454(98)00365-6.
[21] Costa ALM, Reis ACC, Kestens L, et al. Ultra grain refinement and hardening of IF-steel during accumulative roll-bonding. Mater Sci Eng A. 2005;406(1-2):279–285. doi: 10.1016/j.msea.2005.06.058.
[22] Zhilyaev AP, Nurislamova GV, Kim BK, et al. Experimental parameters influencing grain refinement and microstructural evolution during high-pressure torsion. Acta Mater. 2003;51(3):753–765. doi: 10.1016/S1359-6454(02)00466-4.
[23] Ivanisenko Y, Lojkowski W, Valiev RZ, et al. The mechanism of formation of nanostructure and dissolution of cementite in a pearlitic steel during high-pressure torsion. Acta Mater. 2003;51(18):5555–5570. doi: 10.1016/S1359-6454(03)00419-1.
[24] Beladi H, Kelly GL, Shokouhi A, et al. Effect of thermomechanical parameters on the critical strain for ultrafine ferrite formation through hot torsion testing. Mater Sci Eng A. 2004;367(1-2):152–161. doi: 10.1016/j.msea.2003.09.095.
[25] Sauvage X, Wetscher F, Pareige P. Mechanical alloying of Cu and Fe induced by severe plastic deformation of a Cu-Fe composite. Acta Mater. 2005;53(7):2127–2135. doi: 10.1016/j.actamat.2005.01.024.
[26] Belyakov A, Sakai T, Miura H, et al. Substructures and internal stresses developed under warm severe deformation of austenitic stainless steel. Scr Mater. 2000;42(4):319–325. doi: 10.1016/S1359-6462(99)00353-X.
[27] Lianxi H, Yuping L, Erde W, et al. Ultrafine grained structure and mechanical properties of an LY12 Al alloy prepared by repetitive upsetting-extrusion. Mater Sci Eng A. 2006;422(1-2):327–332. doi: 10.1016/j.msea.2006.02.014.
[28] Ning H, Li X, Meng L, et al. Amperometric vitamin C biosensor based on the immobilization of ascorbate oxidase into the biocompatible sandwich-type composite film. Appl Biochem Biotechnol. 2023;167(7):2023–2038. doi: 10.1080/10667857.2023.2172991.
[29] Guo L, Su X, Dai L, et al. Strain ageing embrittlement behaviour of X80 self-shielded flux-cored girth weld metal. Mater Technol Adv Perform Mater. 2023;38(1):2164978. doi: 10.1080/10667857.2023.2164978.
[30] Yang C, Xu H, Wang Y, et al. Hot tearing analysis and process optimisation of the fire face of Al-Cu alloy cylinder head based on MAGMA numerical simulation. Mater Technol. 2023;38(1):2165245. doi: 10.1080/10667857.2023.2165245.
[31] Li Q, Zuo H, Feng J, et al. Strain rate and temperature sensitivity on the flow behaviour of a duplex stainless steel during hot deformation. Mater Technol Adv Perform Mater. 2023;38(1):2166216. doi: 10.1080/10667857.2023.2166216.
[32] Misra RDK, Injeti YSY, Somani MC. The significance of deformation mechanisms on the fracture behavior of phase-reversion induced nanostructured austenitic stainless steel. Sci Rep. 2018;8(1):7908. 1-13. doi: 10.1038/s41598-018-26352-1.
[33] Misra RDK, Challa VSA, Venkatsurya PKC, et al. Interplay between grain structure, deformation mechanisms, and austenite stability in phase reversion-Induced nanograined/Ultrafine-Grained ferrous alloy. Acta Mater. 2015;84:339–348. doi: 10.1016/j.actamat.2014.10.038.
[34] Misra RDK, Nayak S, Mali S, et al. On the significance of nature of strain-induced martensite on phase-reversion induced nano grained/ultrafine-grained (NG/UFG) austenitic stainless steel. Metall Mater Trans A. 2015;41(1):3–12. doi: 10.1007/s11661-009-0072-2.
[35] Misra RDK, Thein-Han WW, Pesacreta TC, et al. Favorable modulation of Pre-Osteoblasts response to nanograined/ultrafine-grained structures in austenitic stainless steel. Adv Mater. 2009;21(12):1280–1285. doi: 10.1002/adma.200802478.
[36] Misra RDK, Thein-Han WW, Pesacreta TC, et al. Cellular response of Pre-Osteoblasts to nanograined/ultrafine-grained structures. Acta Biomater. 2009;5(5):1455–1467. doi: 10.1016/j.actbio.2008.12.017.
[37] Misra RDK, Thein-Han WW, Pesacreta TC, et al. Cellular biological significance of nanograined/ultrafine-grained structures: interaction with fibroblasts. Acta Biomater. 2010;6(8):3339–3348. doi: 10.1016/j.actbio.2010.01.034.

[38] Misra RDK, Thein-Han WW, Mali SA, et al. Cellular activity of bioactive nanograined/ultrafine-grained materials. Acta Biomater. 2010;6(7):2826–2835. doi: 10.1016/j.actbio.2009.12.017.

[39] Venkatsurya PKC, Thein-Han WW, Misra RDK, et al. "Advancing Nanograined/Ultrafine-grained Structures for Metal Implant: interplay between Grooving of Nano/Ultrafine Grains and Cellular R. Materials Science and Engineering C. 2010;30(7):1050–1059. doi: 10.1016/j.msec.2010.05.008.

[40] Misra RDK, Thein-Han W, Somani MC, et al. Phase reversion induced nanograined/ultrafine-grained structures in austenitic stainless steel and their significance in modulating cellular response: biochemical and morphological study with fibroblasts. Adv Eng Mater. 2009;11(12):B235. 242. doi: 10.1002/adem.200900164.

[41] Lowe TC, Reiss RA, Illescas PE, et al. Effect of surface grain boundary density on preosteoblast proliferation on titanium. Mater Res Lett. 2020;8(6):239–246., doi: 10.1080/21663831.2020.1744758.

[42] Saux GL, Magneau A, Gunanrathan K. Spacing of integrin ligands influences signal transduction in endothelial cells. Biophysics Journal. 2011;101:764–773.